

Volume electron microscopy reveals human retinal mitochondria that align with reflective bands in optical coherence tomography [Invited]: supplement

DEEPAYAN KAR,¹  YEON JIN KIM,² ORIN PACKER,² MARK E. CLARK,¹ DONGFENG CAO,¹ CYNTHIA OWSLEY,¹ DENNIS M. DACEY,² AND CHRISTINE A. CURCIO^{1,*}

¹*Department of Ophthalmology and Visual Sciences, Heersink School of Medicine, University of Alabama at Birmingham, Birmingham, AL, USA*

²*Department of Biological Structure, University of Washington, Seattle, WA, USA*

*christinecurcio@uabmc.edu

This supplement published with Optica Publishing Group on 27 September 2023 by The Authors under the terms of the [Creative Commons Attribution 4.0 License](#) in the format provided by the authors and unedited. Further distribution of this work must maintain attribution to the author(s) and the published article's title, journal citation, and DOI.

Supplement DOI: <https://doi.org/10.6084/m9.figshare.24032412>

Parent Article DOI: <https://doi.org/10.1364/BOE.501228>

SUPPLEMENTAL DOCUMENT

Table of Contents

| | |
|---|----|
| Table S1. Donor eyes used for cytochrome c oxidase (COX4) immunohistochemistry. | 2 |
| Fig. S1. Retinal deep capillary overlying rod and cone photoreceptor terminals. | 3 |
| Fig. S2. Near infrared reflectance (NIR) and high-resolution optical coherence tomography (OCT) imaging of 10 healthy human eyes. | 4 |
| Fig. S3. Pericyte mitochondrial morphology in the retinal vascular plexuses. | 5 |
| Visualization 1. Saturated reconstruction of mitochondria in the human outer plexiform layer. | 6 |
| Visualization 2. Three-dimensional demonstration of neuronal mitochondrial distribution in the outer plexiform and inner nuclear layers. | 7 |
| Visualization 3. Serial section EM highlighting mitochondria in neurons of the outer plexiform layer. | 8 |
| Visualization 4. Three-dimensional reconstructions of the mitochondria in outer plexiform layer neurons and vasculature. | 9 |
| Visualization 5. Mitochondria within cone photoreceptors and bipolar neurons adjacent to a retinal capillary. | 10 |
| Visualization 6. Complex mitochondrial morphology of a retinal deep capillary pericyte. | 11 |

Table S1. Donor eyes used for cytochrome c oxidase (COX4) immunohistochemistry.

| Figure | Age | Sex | Eye | D-P time, hours | Eccentricity from fovea, μm | Histologic diagnosis | Relevant medical history |
|---------|-----|--------|------|-----------------|--|----------------------|---|
| Fig. 1A | 94 | female | left | 3.78 | 1839 | nvAMD | Hypertension, osteoporosis, gastroesophageal reflux disease, skin cancer, scoliosis, atrial fibrillation, thyroid disease, renal cyst |
| Fig. 1B | 90 | female | left | 3.80 | 1898 | nvAMD | High blood pressure, cerebral vascular accident, chronic kidney disease, pneumonia |
| Fig. 1C | 83 | female | left | 3.75 | 2864 | Unremarkable | Cardiac pacemaker and valve disorder, hypertension, hypercholesterolemia |
| - | 84 | male | left | 4.05 | 1740 | Unremarkable | Atrial fibrillation, coronary artery disease, hyperlipidemia, hypertension, myocardial infarct, cerebrovascular disease, transient ischemic attack |
| - | 89 | female | left | 5.48 | 312 | Unremarkable | Transient ischemic attack, pneumonia, chronic obstructive pulmonary disease, atrial fibrillation, hyperkalemia, myocardial infarct, urinary tract infection, cardiomegaly, renal disease; former smoker |
| - | 80 | female | left | 4.82 | 2920 | Unremarkable | Hypertension, atrial fibrillation, Gastroesophageal reflux disease |

Mean age 86.7 ± 4.8 years; D-P time, death to processing time; mean D-P time 4.28 ± 0.65 hours; nv, neovascular; AMD, age-related macular degeneration. COX4 distribution in retinal layers was similar across all samples, shown in representative sections in Fig. 1 (A-C). Neovascular lesions were remote from regions shown in figure panels.

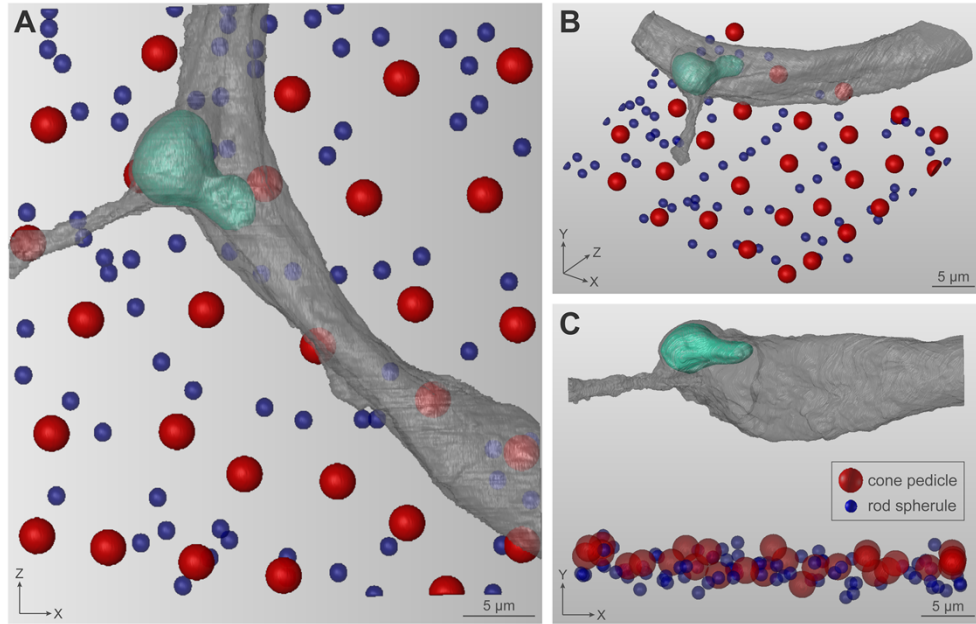


Fig. S1. Retinal deep capillary overlying rod and cone photoreceptor terminals.

Horizontal (A), oblique (B), and vertical (C) views of the OPL show centroids of rod spherules and cone pedicles (shown as blue and red balls, respectively) in a regularly spaced array, 12-14 μm from a branching deep retinal capillary (gray). A pericyte is shown in teal. The rod: cone ratio in this region was estimated as 2.7:1 (50,257 rods per mm^2 and 18,516 cones per mm^2 assigning the region of interest at $\sim 800 \mu\text{m}$ retinal eccentricity, in the parafovea (sampling region dimensions $42.1 \times 35.9 \mu\text{m}$).

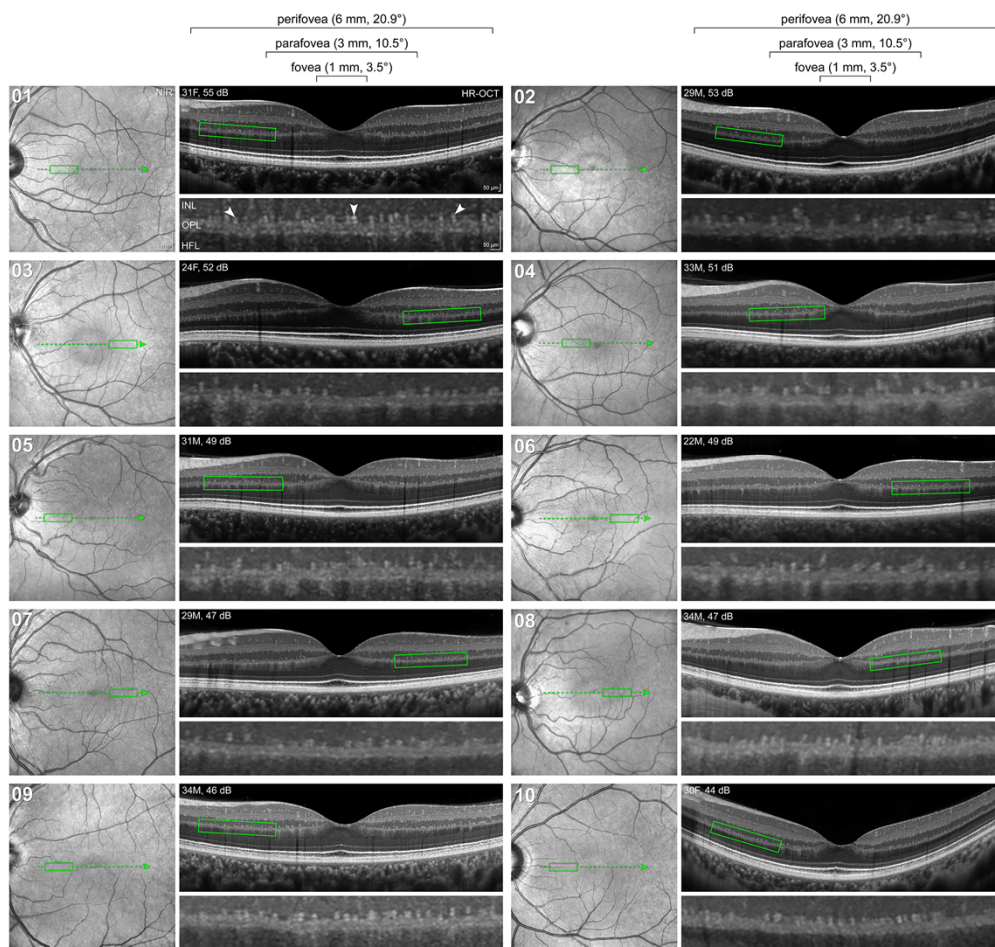


Fig. S2. Near infrared reflectance (NIR) and high-resolution optical coherence tomography (OCT) imaging of 10 healthy human eyes.

Demographic and imaging characteristics of participants are provided in Table 1. NIR image of the fundus shows the sampling location of the cross-sectional OCT scans through the fovea (dotted line, with arrow representing the scan direction). Magnified view of the outer plexiform layer (corresponding to green rectangle) shows presence of outer plexiform layer laminations in all 10 eyes. Visibility of OPL laminations depended on OCT signal-to-noise ratios (in decibels), arranged in order from strongest (upper left) to weakest (lower right). All eyes are shown as left. M, male; F, female. Scale bars: NIR, 1 mm; OCT, 50 μ m.

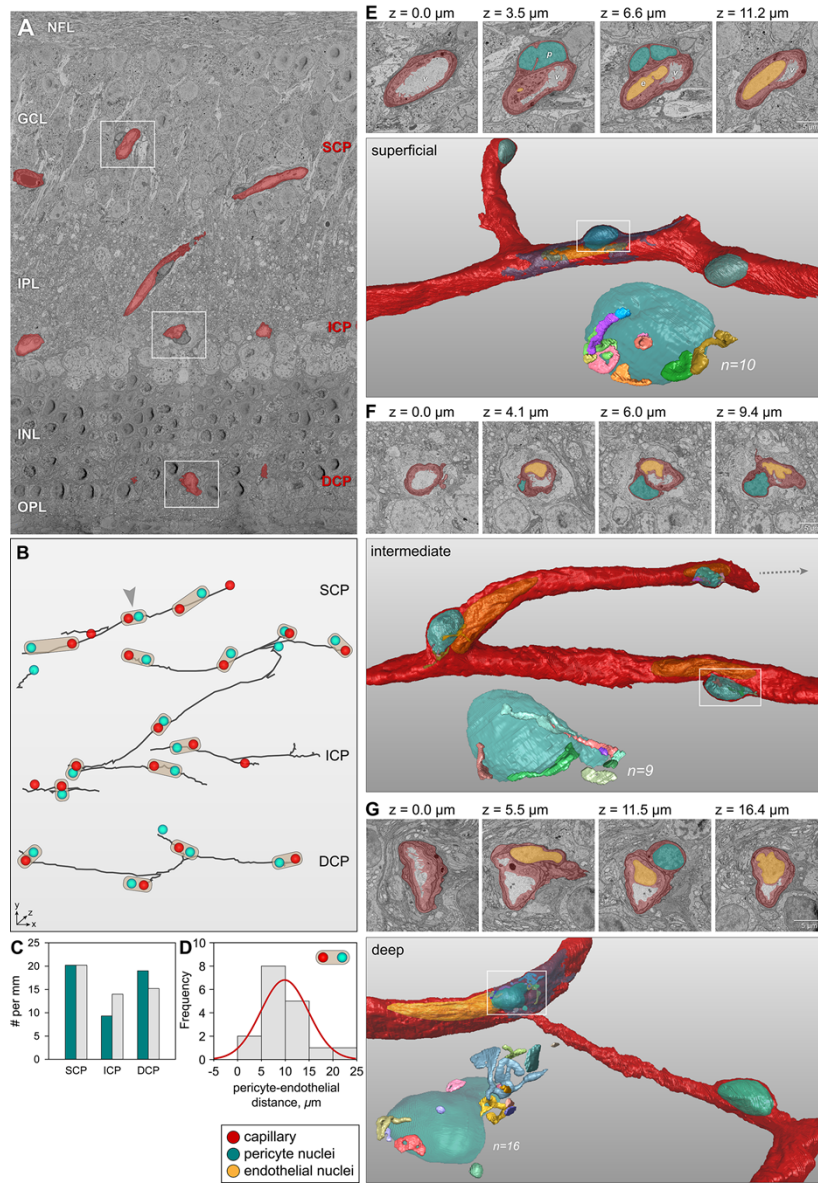
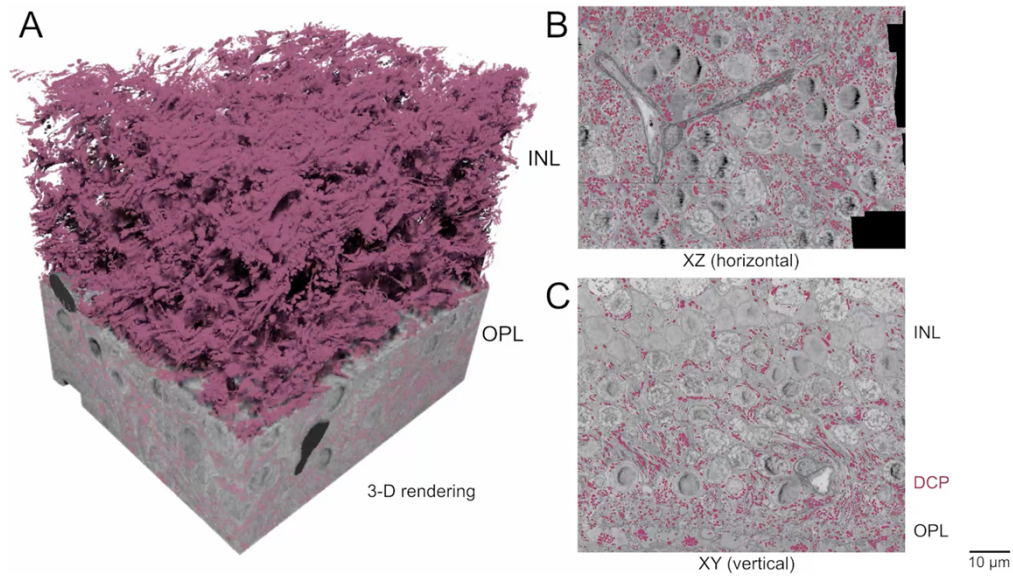


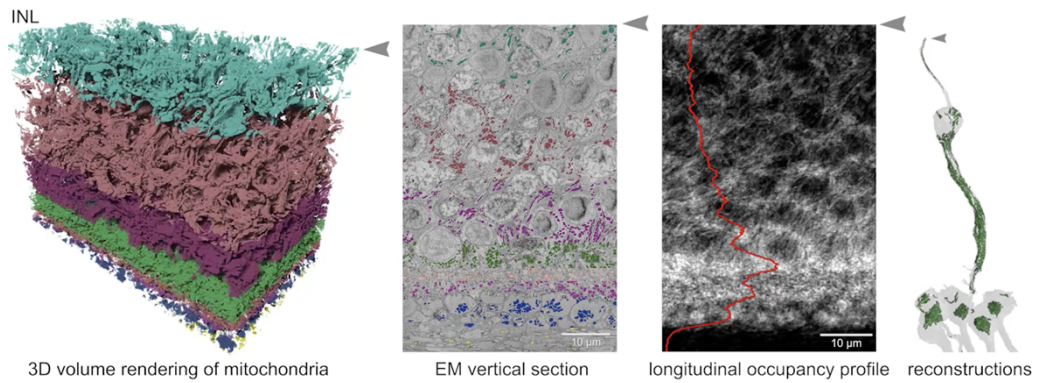
Fig. S3. Pericyte mitochondrial morphology in the retinal vascular plexuses.

A. Representative vertical EM section highlighting the trilaminar vascular plexuses of the retina (red). B. Coupled arrangement of pericyte and vascular endothelial cell nuclei locations is shown in the vessel skeleton map. C. Boxplot shows that the number of pericyte and vascular endothelial cells are relatively similar in the superficial plexus compared to the intermediate and deep plexuses. D. Frequency distribution of pericyte-to-endothelial cell distances. E. Reconstructs of the vascular wall (red), pericyte nuclei (teal), and endothelial nuclei (yellow) in representative plexuses are shown in 3D renderings and in z-stacks of sections from serial block face scanning electron microscopy. Note the mitochondria surrounding the pericyte nuclei.



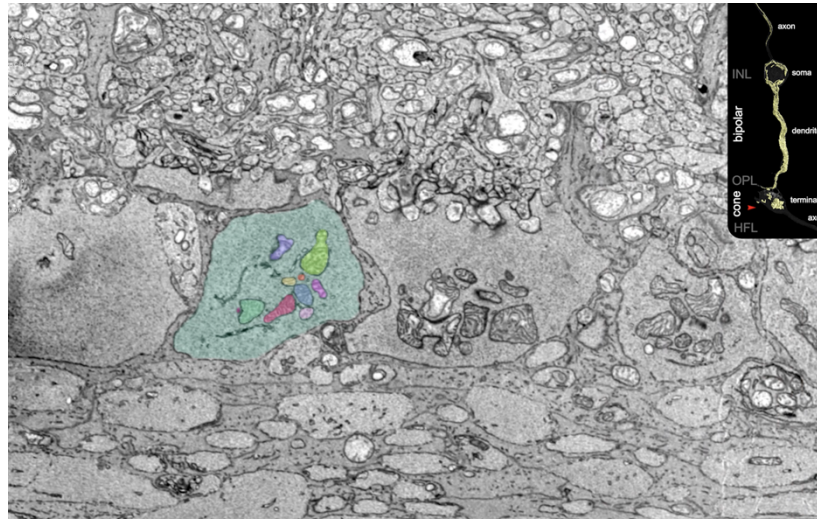
Visualization 1. Saturated reconstruction of mitochondria in the human outer plexiform layer.

Multidimensional views of a volume encompassing the inner nuclear and outer plexiform layers of a human retina with mitochondria labeled in pink. Semantic segmentation was performed on a ~75 GB volume comprising of 925 vertical sections (voxel size 5 x 5 x 50 nm), using a U-Net deep learning model trained to identify mitochondria from the background. Overall, mitochondria occupied 7.9% (33,696 μm^3) of the volume of the tissue block. The performance of the model is shown in Fig. 2.



Visualization 2. Three-dimensional demonstration of neuronal mitochondrial distribution in the outer plexiform and inner nuclear layers.

Multidimensional views highlight the laminar distribution of outer plexiform layer (OPL) and inner nuclear layer (INL). Arrowheads correspond to retinal depths in 3D volume rendering, vertical EM section, longitudinal occupancy profile overlaid on projection image, and representative depth-match mitochondria (green) and OPL neurons (gray) reconstructions (left to right).



Visualization 3. Serial section EM highlighting mitochondria in neurons of the outer plexiform layer.

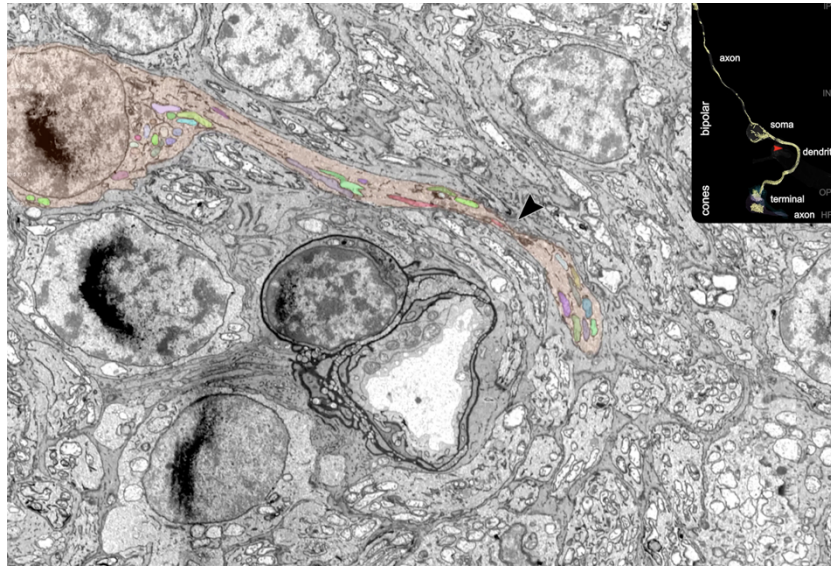
Annotated vertical sections show complete reconstructions of mitochondria in distinct colors occupying a cone bipolar interneuron (orange) receiving input from a cone photoreceptor (teal). Insert in upper right shows 3D reconstructions highlighting mitochondrial content (yellow) in neurons involved in this circuit. Red arrowhead shows the approximate depth corresponding to EM section. (00:00-00:04) Highlighted cone bipolar axon contains long mitochondria occupying the axonal length up to bipolar soma. (00:05-00:20) Fewer mitochondria surround the bipolar nuclei in the somatic compartment. (00:21-00:52) The dendritic compartment is packed with long and slender mitochondria comprising a substantial volume of the neuropil. (00:53-01:17) Mitochondrial clusters occupy individual cone pedicles (photoreceptor terminals). (00:59-01:01) The highlighted cone telodendrion contacts a rod spherule. (01:17-01:29) The photoreceptor axon (surrounded by Müller glia) contains few mitochondria. Sampled region is approximately 60 μm from a retinal capillary from the parafoveal region of a 21-year-old male.



Visualization 4. Three-dimensional reconstructions of the mitochondria in outer plexiform layer neurons and vasculature.

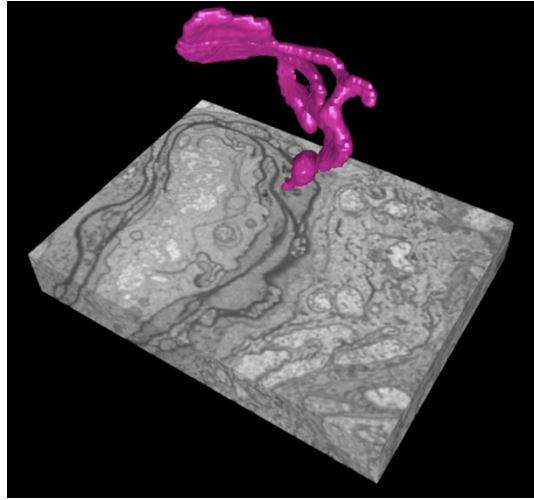
Renderings of complete reconstructions of neurons, mitochondria, and vasculature showing the compartmentalized distribution and morphology of mitochondria network associated with the circuitry comprising the outer plexiform layer. Each mitochondrion used for quantitative analysis is of a distinct color.

- (00:00-00:04) Deep capillary (gray), pericyte nuclei (teal), processes (orange)
- (00:05-00:08) Rod photoreceptors (magenta and purple)
- (00:09-00:16) Cone pedicles
- (00:17-00:27) Two midsize bipolar postsynaptic contacts
- (00:30-00:31) Pericyte mitochondria
- (00:31-00:32) Mitochondria in rod spherules
- (00:32-00:38) Mitochondria clusters in cone pedicles
- (00:39-00:43) Mitochondria in bipolar interneurons.



Visualization 5. Mitochondria within cone photoreceptors and bipolar neurons adjacent to a retinal capillary.

Serial section EM. Annotated vertical sections show the distinct distribution and morphology of mitochondria in two cone pedicles (purple and teal) contacting a bipolar interneuron (orange) encircling a retinal capillary in the outer plexiform layer. Insert in upper right shows mitochondrial content (yellow) in neurons involved in this circuit. Red arrowhead shows the approximate corresponding EM section. (00:06-00:11) Highlighted cone bipolar axon contains 1-2 long mitochondria occupying the axonal length up to bipolar soma. (00:12-00:20) Fewer mitochondria surround the bipolar nuclei in the somatic compartment. (00:20-00:58) The mitochondrial morphology reflects the curvilinear bipolar dendritic course around the capillary. Note the synaptic contacts between the bipolar dendrites and cone pedicles. (00:59-01:01 and 01:07-01:12) The synaptic contacts are characterized by an electron dense region between the processes. (01:01-1:28) Mitochondrial clusters occupy individual cone pedicles (photoreceptor terminals). (01:12-01:31) The photoreceptor axon (surrounded by Müller glia) contains little to no mitochondria. Sampled SBF-SEM serial sections from the parafoveal region of a 21-year-old male retina.



Visualization 6. Complex mitochondrial morphology of a retinal deep capillary pericyte.

3D rendering of a pericyte mitochondria of a deep capillary exhibiting a convoluted shape. The mitochondrial loops and extensions follow the course of the pericyte processes wrapping the vessel lumen.